Glycine-rich peptides from fermented Chenopodium formosanum sprout as an antioxidant to modulate the oxidative stress

Recommended Citation

Hsieh, Chen-Che; Yu, Shu-Han; Kuo, Hsing-Chun; Khumsupan, Darin; Huang, Hsiao-Chu; Liou, Yu-Wei; Kao, Chen-Yu; Shen, Szu-Chuan; and Cheng, Kuan-Chen (2023) "Glycine-rich peptides from fermented Chenopodium formosanum sprout as an antioxidant to modulate the oxidative stress," *Journal of Food and Drug Analysis*: Vol. 31 : Iss. 4 , Article 5.
Available at: https://doi.org/10.38212/2224-6614.3476

Glycine-rich peptides from fermented *Chenopodium formosanum* sprout as an antioxidant to modulate the oxidative stress

Chen-Che Hsieh [a,1], Shu-Han Yu [a,1], Hsing-Chun Kuo [b,h,i,j], Darin Khumsupan [a], Hsiao-Chu Huang [c], Yu-Wei Liou [c], Chen-Yu Kao [d], Szu-Chuan Shen [e], Kuan-Chen Cheng [a,c,f,g,*]

[a] Institute of Biotechnology, National Taiwan University, No. 1, Sec. 4, Roosevelt Rd., Taipei, Taiwan
[b] Division of Basic Medical Sciences, Department of Nursing, Chang Gung University of Science and Technology, Chiayi, Taiwan
[c] Institute of Food Science Technology, National Taiwan University, No. 1, Sec. 4, Roosevelt Rd., Taipei, Taiwan
[d] Graduate Institute of Biomedical Engineering, National Taiwan University of Science and Technology, Taipei, Taiwan
[e] Undergraduate and Graduate Programs of Nutrition Science, School of Life Science, National Taiwan Normal University, Taipei, Taiwan
[f] Department of Optometry, Asia University, 500, Lioufeng Rd., Wufeng, Taichung, Taiwan
[g] Department of Medical Research, China Medical University Hospital, China Medical University, 91, Hsueh-Shih Road, Taichung, Taiwan
[h] Research Fellow, Chang Gung Memorial Hospital, Chiayi 613016, Taiwan
[i] Research Center for Food and Cosmetic Safety, College of Human Ecology, Chang Gung University of Science and Technology, Taoyuan 333324, Taiwan
[j] Chronic Diseases and Health Promotion Research Center, Chang Gung University of Science and Technology, Chiayi 613016, Taiwan

Abstract

Rhizopus oligosporus was utilized in the solid-state fermentation of *Chenopodium formosanum* sprouts (FCS) in a bioreactor. Subsequently, the antioxidant activity of food proteins derived from FCS was investigated. Results showed that glycine-rich peptide (GGGGGKP, G-rich peptide), identified from the <2 kDa FCS proteins, had antioxidant values. According to SwissADME, AllerTOP, ToxinPred, and BIOPEP-UWM analyses, G-rich peptide was identified as safe, non-toxic, and non-allergenic. Afterward, the peptide was examined using *in silico* and *in vitro* studies to evaluate its potential alleviating oxidative stress caused by particulate matter. This study proposed plausible mechanisms that involve the binding of G-rich peptide which inhibited phosphorylation of the v-rel avian reticuloendotheliosis viral oncogene homolog A (RELA) subunit on NF-κB pathway. The inhibition then resulted in down regulation of NF-κB transcription and genetic expression of inflammatory responses. These findings suggested that G-rich peptide from FCS proteins can potentially alleviate oxidative stress.

Keywords: Antioxidant, *Chenopodium formosanum*, Food-derived peptide, Glycine-rich peptide, NF-κB pathway

1. Introduction

Chenopodium formosanum (Djulis) is a native annual herbaceous and pseudocereal plant in Taiwan. Although it shares similar traits with quinoa, *C. formosanum* stands out for its exceptional nutritional value characterized by essential amino acids, phenols, flavonoids, and γ-aminobutyric acid [1,2]. Additionally, *C. formosanum* contains several bioactive compounds such as betanin, kaempferol, and rutin that offer various health benefits associated with lowering hypertension levels and preventing obesity or colon carcinogenesis, among other things [3,4]. Most studies on *C. formosanum* have focused on its phenolic compounds, while limited research has been conducted on its proteins. According to a recent investigation, quinoa protein is an excellent precursor of bioactive peptides with nutritional value and biological activities that promote health benefits. These benefits are released during proteolysis, such as germination,

* Corresponding author at: Institute of Biotechnology, National Taiwan University, No. 1, Sec. 4, Roosevelt Rd., Taipei, Taiwan.
E-mail address: kccheng@ntu.edu.tw (K.-C. Cheng).
[1] Chen-Che Hsieh and Shu-Han Yu equally contributed to the work as the co-first authors.

fermentation, and gastrointestinal digestion [2,5]. Hence, the primary method to prepare bioactive proteins from quinoa protein is enzymatic hydrolysis, which involves microbial fermentation and germinated bioconversion. Then, the hydrolysate resulting from this process can be assessed for its biological activity, including its ability to inhibit angiotensin I conversion and exhibit antioxidant effects [6,7,8]. Despite not being as potent as synthetic drugs, food protein derived peptides (FPPs) display bioactivity, and their accumulation is rare. Moreover, the human body excretes them without any side effects [9]. Dietary nutraceuticals derived from FPPs with antioxidant and anti-inflammatory activity can help maintain redox homeostasis and attenuate oxidative stress [10,11]. With the ongoing air pollution issue that typically induces oxidative stress, it is worth investigating FPPs and their high bioactive properties, which have the potential to mitigate oxidative stress caused by air pollutants.

Particulate matter (PM) is a class of air pollutants that adversely affects respiratory health, which stimulated the presentation of nuclear factor kappa-B (NF-κB) elevated in RAW 254.7 cells [12]. PM-induced oxygen proteases and radicals can activate NF-κB, causing degradation of proteasomal and p50/p65 dimer translocation. Subsequently, the p65 RELA subunit becomes phosphorylated, producing inflammatory cytokines [13,14,15].

In this investigation, it was discovered that glycine-rich protein (GRP) plays a significant role in enhancing antioxidant capacity. However, despite their importance, specific functions of these proteins have not been fully elucidated. Notably, glycine-rich regions are characterized by semi-repetitive glycine-rich motifs that exhibit extraordinary flexibility, similar to a velcro-like mechanism that facilitates protein interactions. As a result, glycine-rich motifs hold great promises as candidates that form functional synergies with other proteins and macromolecules. This is because they promote precise molecular interactions by assuming specific structural conformations [16,17]. Although studies of GRPs and their antioxidant properties in plants are limited, emerging research have shed light on the modulation of plant pathogens by GRPs which prompt a hypothesis regarding their role in plant defense mechanisms. Notably, investigations involving *Capsella bursa-pastoris* roots revealed the isolation of two glycine-rich peptides (referred to as GGH-) that exhibited potent activity against a range of bacterial and fungal strains. Furthermore, in-depth studies of *Triticum kiharae* seeds led to the identification of eight proteins that showed potential fungicidal properties. These findings contribute to the growing body of evidence which supports the involvement of GRPs in plant defense responses against microbial threats [18,19].

This study aims to establish a protocol for extracting FPPs from FCS. After that, FPPs will be evaluated for their anti-inflammation activity using a PM-induced MH-S alveolar macrophage model. The study employs the molecular cut-off (MWCO) extraction method to extract protein fractions in FCS and evaluates the antioxidant ability. The protein fraction with a molecular weight (MW) below 2 kDa is selected for further purification and identification. *In silico* calculations are used to interpret the drug-likeness and predict potential bioactivity of identified FCS proteins. Finally, using bioinformatics tools and immunoblotting, their attenuating effects on PM-induced inflammation are investigated, and the corresponding mechanisms are proposed.

2. Material and methods

2.1. Materials

C. formosanum grains were obtained from Quinoa Green Biotech Co., Ltd (Taichung, Taiwan). *Rhizopus microspores* var *oligosporus* BCRC 31996 and murine alveolar macrophage MH-S cell line were sourced from Bioresource Collection and Research Center (BCRC) (Hsinchu, Taiwan). Agar, potato dextrose broth, and peptone, which constitute the medium, were acquired from BioShop Canada Inc (Ontario, Canada). Superdex 30 Increase SEC columns, Sephadex G-25 columns resin, Penicillin/streptomycin and trypsin EDTA solution, used for protein purification and cell culture, were procured from GE Healthcare Life Science (Logan, Utah, USA). Vivaspin 15R and Vivaspin Turbo 15 were obtained from Sartorius Stedim Biotech GmbH (Goettingen, Germany). GIBCO Life Technologies (Grand Island, USA) supplied the cell culture mediums and fetal bovine serum. Immunoblot-related materials, namely RIPA buffer (10X), phosphor-p65, beta-actin, and p65 antibody, were purchased from Cell Signaling Technology (Beverly, MA, USA). TBST Buffer, Transfer Buffer, ECL substrate, and protein assay dye reagent were obtained from Bio-Rad Laboratories, Inc. (Hercules, CA, USA). Goat anti-rabbit IgG antibodies (HRP) were acquired from Genetex (Irvine, CA, USA). All the chemicals utilized in the research were of analytical grade and were procured from Merck (Burlington, MA, USA).

2.2. Preparation of C. formosanum sprouts fermentation

In the bioreactor (FS−V-SA05P, Major Science, Taoyuan, Taiwan), 1.5 kg of *C. formosanum* sprouts

were introduced and sterilized for 20 min at 121 °C. Afterward, 75 mL of *Rhizopus oligosporus* spores at a concentration of 10^6 spores/mL (5% (v/w)) were inoculated onto the substrate. The solid-state fermentation process was conducted at 35 °C with 0.4 vvm (air volume/culture volume/min) aeration volume and a rotation speed at 5 rpm for four days [2].

2.3. MWCO protein extraction of fermented C. formosanum sprouts (FCS) product

The lyophilized FCS was ground into powder and sieved through a 30-mesh screen prior to storage at −20 °C. Subsequently, degreasing was carried out using n-hexane (1:3 w/v) at 37 °C for 2 h. The resulting mixture was collected and dried using a rotary vacuum evaporator (HC scientific and instrument, Taipei, Taiwan) to obtain degreased FCS sample, which was then mixed with phosphate-buffered saline (1:10 w/v) and homogenized. The homogenized sample was centrifuged at $15,000 \times g$ for 30 min at 4 °C to collect the supernatant, which was then heated at 70 °C to inactivate enzyme activity. Following a protein extraction method [20], ammonium sulfate was incrementally added to the FCS supernatant until a 90% saturation concentration was achieved. The resulting salting-out sample was then centrifuged at $15,000 \times g$ for 30 min at 4 °C to collect the protein precipitation. FCS protein precipitation was further carried out using Vivaspin 15R and Vivaspin Turbo 15 according to the manufacturer's instructions to obtain three fractions: below 2 kDa, 2–10 kDa, and above 10 kDa. The FCS protein fractions were obtained by centrifugation at $6,000 \times g$ for 30 min at 4 °C. After desalting, different molecular FCS protein fractions were freeze dried and stored at −20 °C for further experiments.

2.4. Isolation of G-rich peptide from FCS proteins

The FCS protein fractions were purified according to the method by Liu et al. (2015) [21], which used fast protein liquid chromatography (ÄKTA purifier UPC 10, GE Healthcare Life Science, Utah, USA) with a series of five 5 mL HiTrap desalting columns (prepacked with Sephadex G-25 superfine, GE Healthcare Life Science) equilibrated with distilled water at a flow rate of 2 mL/min and monitored at 280 nm. FCS protein fractions were collected and reconstituted with distilled water. The purified G-rich peptide protocol was modified as described by Ngo et al. (2015) [22], which was equipped with Superdex 30 Increase SEC columns (prepacked Tricorn™ glass column, GE Healthcare Life Science) and equilibrated with distilled water at a flow rate of

0.5 mL/min. Meanwhile, Gly–Tyr, Leu enkephalin, Met enkephalin, and Val-Tyr-Val (Merck, Burlington, MA, USA) were used as standards to detect the G-rich peptide on FPLC profiling. FCS protein fractions and G-rich peptide were freeze dried and stored at −20 °C until further experimentation.

2.5. Identification of G-rich peptide from FCS proteins

The peptides were analyzed according to the methods [23,24], with services provided by BIO-TOOLS Biotechnology Co., Ltd. (Taipei, Taiwan). Briefly, the peptides were diluted in buffer A (0.1% formic acid) and subjected to separation employing a reverse-phase column (Zorbax 300SB-C18, 0.3×5 mm; Agilent Technologies), followed by an additional separation step which utilized a column (Waters BEH 1.7 μm, 100 μm I.D. $\times$ 10 cm with a 15 μm tip) with a multistep gradient of buffer B (99.9% acetonitrile/ 0.1% formic acid) and a flow rate of 0.3 μL/min for 70 min. The full-scan MS analysis was performed using the Orbitrap mass spectrometer over a mass range of 400–2,000 Da, with a resolution of 120,000 at m/z 400. Internal calibration was accomplished using the ion signal of protonated dodecamethylcyclohexasiloxane ion at m/z 536.165365 as a lock mass. A data-dependent MS/MS acquisition strategy was employed, consisting of 20 MS/MS scan events followed by one MS scan to target the 20 most abundant precursor ions identified in the preview MS scan. The m/z values selected for MS/MS were dynamically excluded for 40s, employing a relative mass window of 15 ppm. For the experimental setup, the electrospray voltage was set to 2.0 kV, and the capillary temperature was maintained at 200 °C. The MS and MS/MS automatic gain control parameters were configured as follows: 1,000 ms (full scan) and 200 ms (MS/MS), or 3×10^6 ions (full scan) and 3,000 ions (MS/MS) for maximum accumulated time or ions, respectively.

The acquired data were subsequently analyzed using Proteome Discoverer software (version 1.4, Thermo Fisher Scientific™), and the MS/MS spectra were searched against the Uniprot database by utilizing the Mascot search engine (Matrix Science, London, UK; version 2.5). For peptide identification, a mass tolerance of 10 ppm was allowed for intact peptide masses, and 0.5 Da for CID fragment ions, with consideration for two missed cleavages resulting from trypsin digestion. The variable modifications considered were oxidized by methionine and acetyl (protein N-terminal), while carbamidomethyl (cysteine) was regarded as a static modification. Peptide-spectrum matches were then filtered based

on high confidence to retain only those with a Mascot search engine rank of 1 for peptide identification, ensuring an overall false discovery rate below 0.01. Proteins with a single peptide hit were retained in the analysis [2].

2.6. Determining antioxidant activity of G-rich peptide and FCS proteins

The free radical scavenging activity using 2,2'-Azino-bis 3-ethylbenzothiazoline-6-sulphonic acid (ABTS) was employed according to the protocol [25]. Briefly, a 7 mM ABTS solution was dissolved in water and mixed with 2.45 mM $K_2S_8O_2$ in equal proportions. The solution was diluted with water to achieve an absorbance of 0.7 at 734 nm. Next, 20 μL of the FCS proteins and 180 μL of diluted ABTS were added to a 96-well plate and incubated for 6 min at room temperature. The absorbance was measured at OD 734, and the ABTS scavenging ability was expressed as Trolox equivalent antioxidant capacity (TEAC) in mM.

2.7. Predicting the ADME, toxicity, allergenicity, and potential bioactivity of a G-rich peptide from FCS protein fractions

In silico methods for drug discovery have the potential to reduce the need for experimental studies and improve success rates. Accordingly, drug-likeness rules were initially applied to screen for oral bioavailability. Then, secondary screening was carried out using the SwissADME (www.swissadme.ch/, accession date – March 13, 2023) online tool to calculate ADME (absorption, distribution, metabolism, and excretion) profiles and assess pharmacokinetic parameters for identification of novel candidate drugs [26]. The ToxinPred server (http://crdd.osdd.net/raghava/toxinpred, accession date – March 14, 2023) [27] was utilized to predict potential toxicity of peptides, while the prediction of allergenicity was conducted using AllerTOP v.2.0 (http://www.ddg-pharmfac.net/AllerTOP, accession date – March 15, 2023) [28]. In addition, BIOPEP-UWM (https://biochemia.uwm.edu.pl/biopep-uwm/, accession date – March 16, 2023) web server was employed to calculate the activity profile of identified peptides [29].

2.8. Preparation of PM solutions and FCS proteins for cell experiments

PM (Diesel - Clay Loam 1, CRM558) was procured from Merck (Burlington, MA, USA). To prepare PM preservation solutions within a concentration range of 200 mg/mL [30], PM was mixed with 1 mL of dimethyl sulfoxide (DMSO), vortexed for 3 min, and sonicated for 1 h prior to storage at −20 °C. Subsequently, freeze dried G-rich peptide and FCS proteins were added to the fresh RPMI-1640 (containing 1% FBS) and diluted to 50, 100, and 200 ppm before storing at −20 °C for later use. Prior to experimentation, the PM solution was sonicated for 30 min and incubated at 37 °C before diluting to the desired concentration.

2.9. Treatment of PM-MHS model

MH-S cells were seeded in 96-well plates with density of 5×10^5 cells/mL. After the cells adhered to the well, the medium was replaced with fresh RPMI-1640 containing 10% FBS, 200 ppm PM, and various concentrations of FCS proteins. The cells were then incubated at 37 °C with 5% CO_2 for 24 h.

2.10. Determination of cell viability

Cell viability was evaluated using the CCK-8 kit (Dojindo Laboratories, Kumamoto, Japan) according to the manufacturer's instructions. Briefly, MH-S cells were incubated with 10% CCK-8 solution for 1 h, followed by measurement of absorbance at OD 450 using a microplate reader (MULTISKAN GO, Thermo Fisher Scientific, Waltham, MA, USA). Cell viability was calculated as the percentage of absorbance of sample over control, using the formula: Cell viability = (OD_{450} Sample/OD_{450} Control) x 100%.

2.11. Determination of reactive oxygen species (ROS)

Dichloro-dihydro-fluorescein diacetate (DCFH-DA), purchased from Merck, was used as fluorescence probes. After incubation, MH-S cells were rinsed with PBS buffer twice and 10 μM DCF-DA probes were added before incubating at 37 °C with 5% CO_2 for 20 min. After incubation, the fluorescence probes were removed, and MH-S cells were washed with PBS buffer twice for fluorometric analysis. Quantification of ROS was measured using a fluorescence microplate reader (Varioskan LUX Multimode Microplate Reader, Thermo) with an excitation wavelength of 488 nm and an emission wavelength of 525 nm. The ROS level in each well was normalized with the control group (100%) and corrected by dividing it with the cell viability [31]. The generation of ROS in cells was observed and captured using a fluorescence microscope (Carl Zeiss Inc., Oberkochen, Germany).

2.12. Transcriptome analysis

In this experiment, cDNA library construction and sequencing analysis were conducted by BIOTOOLS Biotechnology Co., Ltd. (Taipei, Taiwan). High-throughput paired-end 150 bp sequencing analysis was performed using Illumina NovaSeq 6000 (Illumina, San Diego, CA, USA). The expression of each gene was calculated using feature counts and referred from the Mouse Reference Genome (*Mus musculus*)-GRCm38 gene database. Differential expression genes (DEGs) between each treatment group were screened by DESeq2 with biological repeatability, with the values set to log2 fold change ≥ 2 and *p*-value adjusted to ≤ 0.05 for significant difference in Gene Ontology (GO) analysis, as described by An et al. (2021) [32].

2.13. Chromatin immunoprecipitation (ChIP) analysis

In this experimental procedure, MH-S cells were subjected to a treatment involving incubation with 1% formaldehyde at 37 °C which aimed to induce DNA-protein cross-link formation. To halt the cross-linking reaction, glycine (125 mM) was added and allowed to incubate for 5 min. Subsequently, the cells were transferred into a cell lysis buffer and incubated overnight at 4 °C in the presence of p65 antibodies and protease inhibitors. Afterward, the cells underwent a wash step with an elution buffer, and the cross-linking immunoprecipitated complexes were subjected to incubation at 65 °C for a duration of 2 h. The resulting DNA fragments were purified using the ChIP DNA Clean & Concentrator Kit (Zymo, Tustin, CA, USA), and quantitative PCR analysis was performed utilizing specific primers (Table S1) to amplify the promoter region of *iNOS*, *COX2*, *TNFα*, *IL-1β*, and *IL-6* genes. The fold enrichment of the specific genes as well as percentage in ChIP were determined and calculated by employing the calculation method [33].

2.14. Immunoblot

MH-S cells were harvested and washed twice with iced phosphate-buffered saline (PBS) before being centrifuged for 20 min at $12,000\times g$. The protein concentration was measured using a Bradford assay kit (Thermo Scientific™, MA, USA) in accordance with the manufacturer's instructions. Primary antibodies (beta-actin, p-p65, and p65) were used at a 1:1,000 dilution, while secondary antibodies (HRP-conjugated anti-mouse IgG and anti-rabbit IgG) were used at a 1:7,500 dilution. Protein expression was quantified by densitometric analysis using ImageJ.

2.15. Docking technique

Docking was conducted using AutoDock Vina 1.2.3 [34] and the PyMOL visualization tool (DeLano Scientific LLC, San Francisco, CA, USA) was used to analyze the output docking results. The 3D structures of G-rich peptide were obtained from the Alphafold2 [35]. The crystal structure of NF-κB (PDB ID: 1VKF) was retrieved from the Protein Data Bank (http://www.rcsb.org/). Prior to docking simulations, all non-protein molecules were removed, and any alternative atom locations were eliminated, retaining only the required location, and energy was minimized. A grid box of $28.5 \times 34.5 \times 26.25$ (RELA subunit) was created along the XYZ axes, with a grid spacing of 0.375 that spanned the protein structure. The grid center of the RELA subunit was X: -14.63, Y: 54.821, and Z: 63.425.

2.16. Statistical analysis

Experimental measurements were performed in triplicate, and the results were reported as the mean $\pm$ standard deviation. Data processing was conducted using Microsoft Excel 2016, while Sigma-Plot 12.0 (Systat Software, Inc., Chicago, IL, USA) for Windows was employed to carry out Duncan's multiple range and t-tests. Statistical significance was determined at a *p*-value of less than 0.05.

3. Results and discussion

3.1. Determining antioxidant activity of different MW proteins from fermented C. formosanum sprouts (FCS)

Food antioxidant proteins are widely recognized for their health benefits due to their high bioactivity levels [36,37]. This study used the MW cut-off (MWCO) approach to investigate the antioxidant proteins in FCS. All the data were conducted in triplicate to ensure statistical validity. Table S2 shows that FCS proteins with MW below 2 kDa exhibits more robust antioxidant capabilities than those with MW between 2 and 10 kDa and above 10 kDa. Specifically, FCS proteins with MW below 2 kDa have an ABTS value of 0.23 ± 0.01 mM Trolox, which is 1.21 and 2.09 times significantly greater than that of FCS proteins with MW between 2 and 10 kDa and above 10 kDa, respectively. Similarly, another study revealed that quinoa protein hydrolysate with lower MW (<5 kDa) exhibits more potent bioactivity than

that with a higher MW (>5 kDa) [38]. Furthermore, other previous studies consistently demonstrated that low molecular weight (MW) peptides exhibit superior radical scavenging properties compared to their high MW counterparts [37,39,40]. For instance, small MW peptides (900 and 500 Da) from chicken essence fractions, and peptides <600 Da rich in His and Tyr from cod (*Gadus morhua*) protein hydrolysates showed high radical-scavenging activity [41,42,43]. The reduced scavenging power of larger peptides may be attributed to potential steric hindrance resulting from their size and increased peptide repulsion caused by bulkier structures [44]. These findings suggest that lower MW proteins derived from FCS have potential bioactive properties that warrant further investigation.

3.2. Identification of antioxidant peptides from FCS proteins

The study's findings are further supported by the analysis of FCS fractions using fast performance liquid chromatography (FPLC), as demonstrated in Fig. 1A to F. The profiling of below 2 kDa FCS fractions reveals the presence of two distinct peaks, with fraction 2 showing a significant increase in intensity as the fermentation period progresses. In addition, Table S2 indicates that fraction 2 (peak 2 in FPLC profiling) exhibits higher antioxidant properties than fraction 1 (peak 1 in FPLC profiling), with ABTS values of 1.01 ± 0.05 and 0.32 ± 0.04 mM Trolox, respectively. This represents an increase of 3.16 times over fraction 1's antioxidant ability. The results suggest that prolonged fermentation periods can

significantly increase the free peptide content and anti-oxidative ability of FCS products. In a recent study, it is discovered that the free peptide content and anti-oxidative ability of FCS products are significantly improved with prolonged fermentation periods. This enhancement in bioactive properties could be attributed to the microbial hydrolysis of protein structures, which exposes previously hidden amino acids within the parent protein [2].

After using ESI-Q-TOF-MS/MS method and blasting in *Chenopodium* Uniports database, three b-type ions were observed at *m/z* 414.15, 397.16 and 286.04. Meanwhile three y-type ions were also detected at *m/z* 415.23, 397.16 and 301.10. These results represent a peptide with the sequence Gly-Gly-Gly-Gly-Gly-Lys-Pro (GGGGGKP) or Glycine-rich peptide (G-rich peptide). Moreover, the MW was determined which was approximately 529 g/mol (Fig. 1G). In previous studies, a significant proportion of putative chemo-preventive peptides identified from quinoa are found to be fragments of 11S globulin family, which is the major seed storage protein of quinoa. However, the GGGGGKP is a fragment of DEAD-box ATP-dependent RNA helicase 8-like isoform X1 from *Chenopodium quinoa*. Unlike most research that investigates bio-functional properties of 11S globulin from quinoa protein, this study first discovers that GGGGGKP has the antioxidant activity which may be considered as chemo-preventive nutraceuticals. Plant and cereal-derived peptides possess many bioactive properties, including antioxidant, anti-inflammation, anti-hypertensive, and anti-pulmonary fibrosis effects. These peptides from FPPs are characterized by a
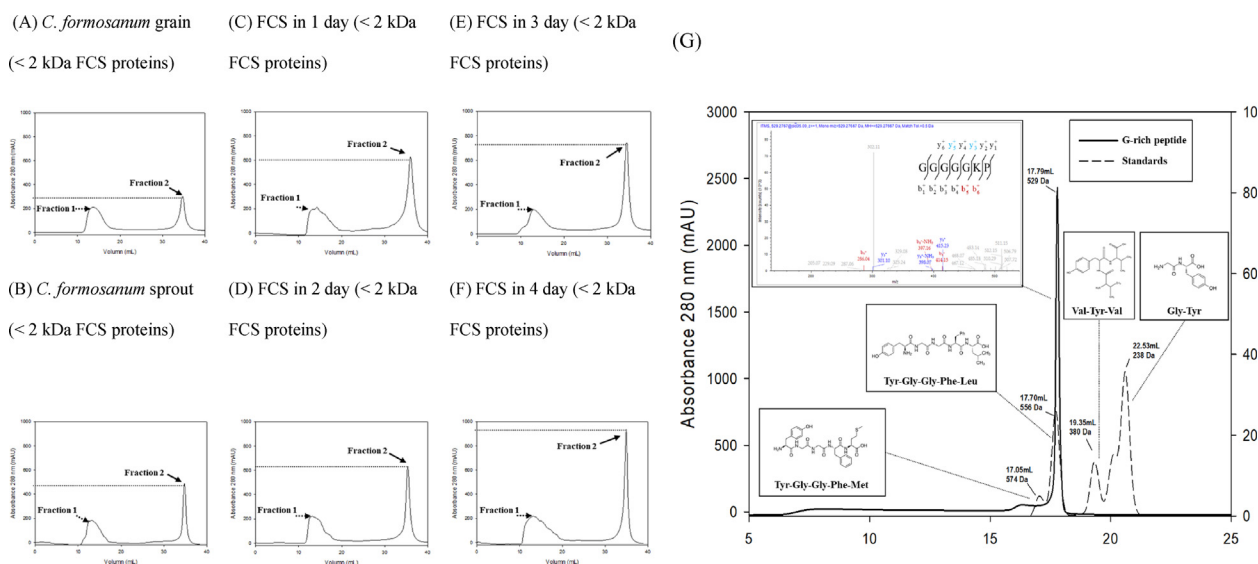

Fig. 1. *Identification and purification of the G-rich peptide from FCS proteins with FPLC and mass spectra. The FPLC profile of <2 kDa FCS proteins during C. formosanum sprout fermentation (A to F); Determination of the G-rich peptide molecular mass (fraction 2) (G).*
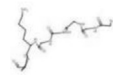
high content of glycine (G), as exemplified by sequences such as GGLGDVLGGLP, GEKGGIPIGIGK, and GEGW from *C. quinoa* protein, broken rice protein, and *Acheta domesticus*. Since they contain antioxidants, they are promising as protective agents against free radicals and oxidative stress [2,10,38,40,44,45,46]. Notably, the antioxidant peptides studied exhibit a common presence of lysine, which contributes to their excellent free radical scavenging properties [43]. The biological activity of peptides often varies significantly and is primarily determined by the amino acid sequence and its configuration and hydrophobicity [47]. Peptides containing cysteine and glycine have been found to possess antioxidant properties by donating protons to free radicals [48].

3.3. In silico study and evaluation of G-rich peptides from FCS proteins

An *in silico* analysis was performed to evaluate the G-rich peptide from other lower MW FCS proteins. The calculated total polar surface area (TPSA) was 234.92 $Å^2$, while the number of rotatable bonds (ROTB) was 22. The peptide has seven hydrogen bond donors (HBD) and nine hydrogen bond acceptors (HBA) (Table 1). Orally available peptide drugs that are FDA-approved can have TPSA for as high as 400 $Å^2$ and around 20 rotatable bonds, with up to 50 HBA and 25 HBD [47]. However, the G-rich peptide violates Lipinski's rule of five by exceeding the recommended MW of 500 g/mol, with more than 10 HBA and an octanol−water partition coefficient above 5. Nevertheless, it is essential to note that many orally available peptide drugs on the market or in clinical trials do not conform to these drug-likeness criteria [49,50]. Therefore, a consideration of similar clinical examples may provide further insights into the feasibility of G-rich peptide from FCS proteins as absorbable nutraceuticals. Another strategy to improve the drug-likeness is by modifying the structure of G-rich peptides, such as reducing the number of rotatable bonds, hydrogen donors, and TPSA. A recent study shows that several modifications, including amidation, acetylation, benzoylation, and benzylation, can be done on N-terminal and C-terminal of the peptide to increase its bioactivity and drug-like property [51]. The modified G-rich peptide from FCS proteins may be an ideal way to improve pharmacokinetic properties in future experiments.

In addition, the pharmacokinetic analysis of G-rich peptide suggested that it has negligible effects on inhibiting xenobiotic metabolism in humans. ToxinPred is a support vector machine model

Table 1. *In silico ADME, toxicity, allergenicity, bioactive, and antioxidant ability profiles of the multifunctional G-rich peptides from FCS proteins.*

Properties	Items	Parameters
Physicochemical	Sequence	GGGGGKP
	Formula	$C_{21}H_{36}N_8O_7$
	Structure	
	Bioavailability Radar	
	Mol. wt.	529 (g/mol)
	ROTB	22 (n)
	HBA	9
	HBD	7
	TPSA	234.92 $Å^2$
Pharmacokinetics	CYP1A2 inhibitor	NO
	CYP2C19 inhibitor	NO
	CYP2C9 inhibitor	NO
	CYP2D6 inhibitor	NO
	CYP3A4 inhibitor	NO
Drug likeness	Lipinski	MW > 500, NorO>10, NHorOH>5
Toxicity	ToxinPred	Non-toxin
Allergenicity	AllerTOP	Non-allergen
Potential bioactive seq.	ACE inhibitor	GG, GK
	Antioxidative	KP
	DPP IV inhibitor	GG, KP

specifically designed to achieve high precision in discriminating between toxic and non-toxic peptides, relying on the peptide's composition of Pro, Asp, and His. AllerTOP, on the other hand, employs machine learning methods for classification by utilizing amino acid E-descriptors, auto- and cross-covariance transformation [27,28]. In this study, both ToxinPred and AllerTOP were applied for *in silico* predictions. The results indicated that the peptide is non-toxic and unlikely to cause allergenic reactions. The G-rich peptide is also found to possess potential bioactive properties such as ACE inhibitor (GG, GK), antioxidative (KP), and DPP IV inhibitor (GG, KP), suggesting that it could potentially be utilized as nutraceuticals in food industries (Table 1).

3.4. In vitro study and evaluation of G-rich peptides to alleviate PM hazards

In vitro assays indicated that the antioxidant ability of FCS proteins corresponds to lower MW. Within this study, the potency of various FCS proteins, including the G-rich peptide, was determined using PM-MHS model. According to ISO 10993−5 [52],
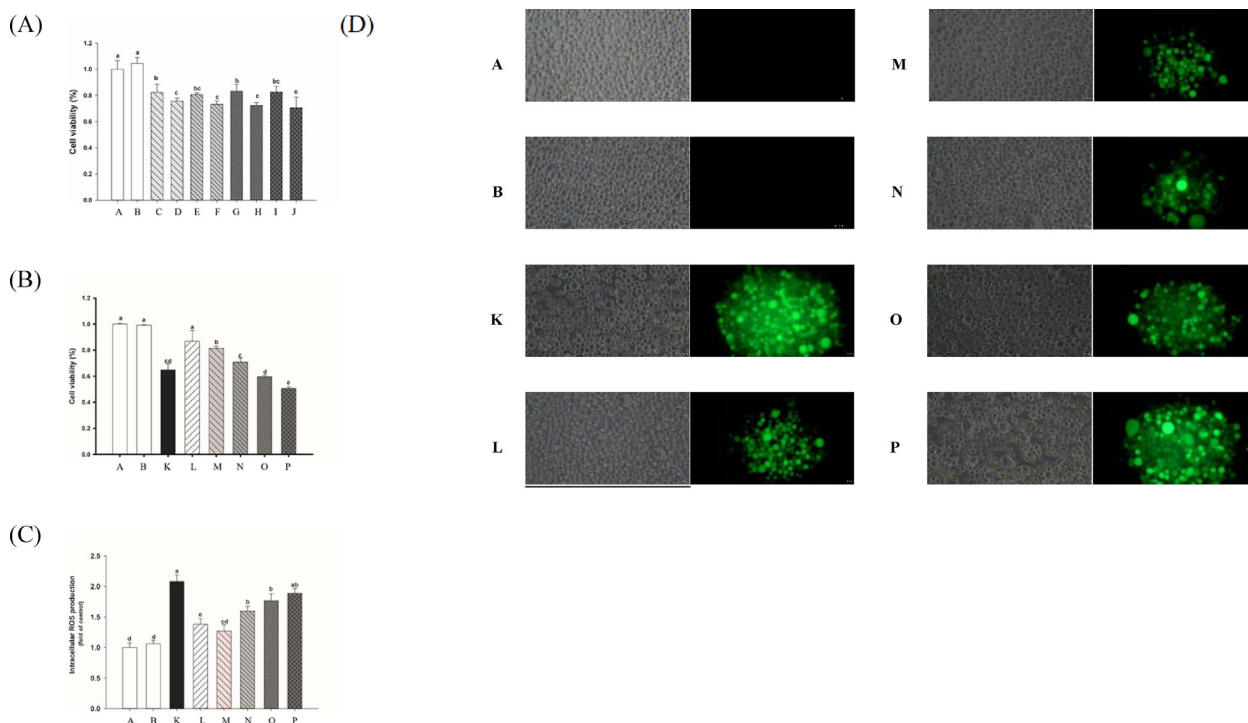
Fig. 2. Effects of FCS proteins on ROS production on PM-MHS model. The toxicity at various doses of FCS proteins (A); The capability of FCS proteins to reduce intercellular ROS production (B); The ability of FCS proteins to restore cell viability (C); Fluorescence images recorded by an inverted fluorescence microscope (400 x) (D). Each value represents means ± SD of triplicates. Different letters a-e in the same column mean significant difference (p < 0.05). A: without treatment; B: treated with only 0.1% DMSO for 24 h; C, D: treated with 100 and 200 ppm G-rich peptide; E, F: treated with 100 and 200 ppm below 2 kDa protein fraction; G, H: treated with 100 and 200 ppm 2−10 kDa protein fraction; I, J: treated with 100 and 200 ppm upon 10 kDa protein fraction; K: treated with 200 ppm PM for 24 h; L: co-treated with 1 mM NAC and 200 ppm PM for 24 h; M: co-treated with 100 ppm G-rich peptide and 200 ppm PM for 24 h; N: co-treated with 100 ppm below 2 kDa protein fraction and 200 ppm PM for 24 h; O: co-treated with 100 ppm 2−10 kDa protein fraction and 200 ppm PM for 24 h; P: co-treated with 100 ppm upon 10 kDa protein fraction and 200 ppm PM for 24 h.

100 ppm FCS proteins are considered non-cytotoxic on the MH-S cells, as illustrated in Fig. 2A. After exposure to PM and treatment with 100 ppm G-rich peptide, cell viability was significantly restored from $64.8 \pm 4.5\%$ to $81.4 \pm 1.6\%$. Furthermore, compared to other FCS proteins, cells treated with G-rich peptides had the highest survival rate (Fig. 2B). Regarding ROS production, the G-rich peptide-treated group showed the highest down-regulation from 2.08 ± 0.11 to 1.27 ± 0.10 times, compared to PM exposure alone. This effect is comparable to that of the 1 mM NAC-treated group (approximately equal to 163 ppm) (Fig. 2C). Additionally, fluorescence images showed that the intensity caused by ROS accumulation significantly declined due to G-rich peptide intervention (Fig. 2D). The inclusion of hydrophobic amino acids within the peptides enhances their hydrophobic solubility, facilitating peptide−peptide interactions and proton donation to radical species. In addition, positively charged amino acids and proline residue with indole and pyrrolidine rings could act as hydrogen donors via their hydroxyl groups [53]. This may explain the antioxidant capability of G-rich peptide and its modulation of ROS production. Furthermore, transcriptomic study from the cell model illustrated that of G-rich peptide resulted in the upregulation of 2280 differentially expression genes (DEGs) and the downregulation of 2476 DEGs compared to the PM-treated only group (Fig. 3A, B). Additionally, the top 5 relevant DEGs, as shown in Fig. 3C, D, were mainly involved in regulating NF-κB signaling and immune-related gene ontology (GO). Also, the Kyoto Encyclopedia of Genes and Genomes database (KEGG) analysis reveals that G-rich peptide could downregulate the expression of many genes in the NF-κB signaling pathways (Fig. 3E, F). Previously studies indicated that PM 2.5-induced ROS production can trigger a number of redox-sensitive signaling pathways which result in diverse biological processes (such as inflammatory, the regulation of cell survival, and proliferation) through the oxidative stress-regulated MAPK/NF-κB pathway [54,55,56]. Consequently, NF-κB signaling pathways may be the most sensitive biological response to PM exposure and G-rich peptide treatment.

Moreover, an investigation of nodal gene expression showed the downregulation of Interleukin

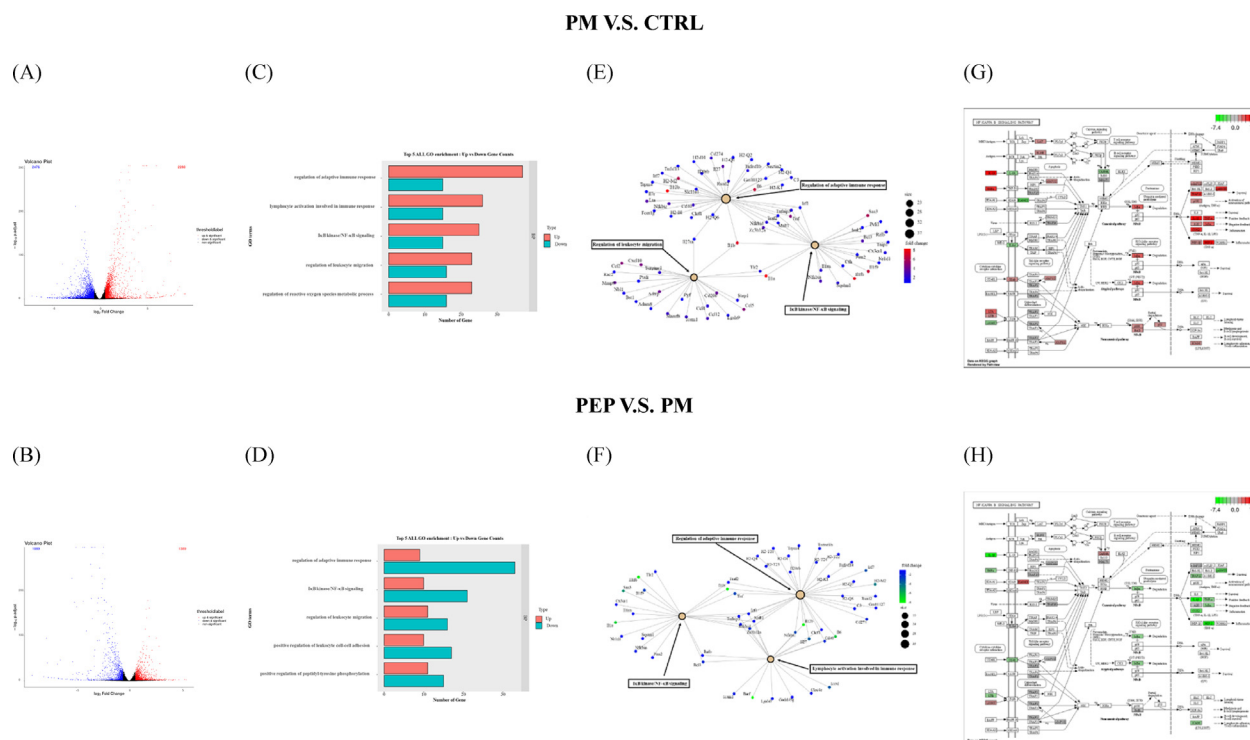**PM V.S. CTRL**

PEP V.S. PM

Fig. 3. Gene Ontology (GO) functional enrichment and Kyoto encyclopedia of genes and genomes (KEGG) analysis of differential expression genes (DEGs) with or without treatment of G-rich peptide from FCS proteins on PM-MHS model. Volcano map (A, B); Up and down gene count in top 5 gene events (C, D); DEGs changing in top 3 gene events (E, F) and KEGG pathway (NF-κB pathway) enrichment of DEGs (G, H). The DEGs with adjusted p-value <0.05 and log2 fold change >1.5 are shown. CTRL: without treatment; PM: treated with only PM (200 ppm) for 24 h; PEP: co-treated with 200 ppm PM and 100 ppm G-rich peptide from FCS proteins for 24 h.

family genes, particularly *IL-1β* (Fig. 3F). The research similar to this study applied GO and KEGG to analyze changes in genetic and signal cascades during PM exposure in macrophage.

Results revealed that C-X-C motif chemokine ligand and interleukin family members were the nodal genes that cause oxidative stress and inflammatory responses [32]. Furthermore, Fig. 1S illustrates that
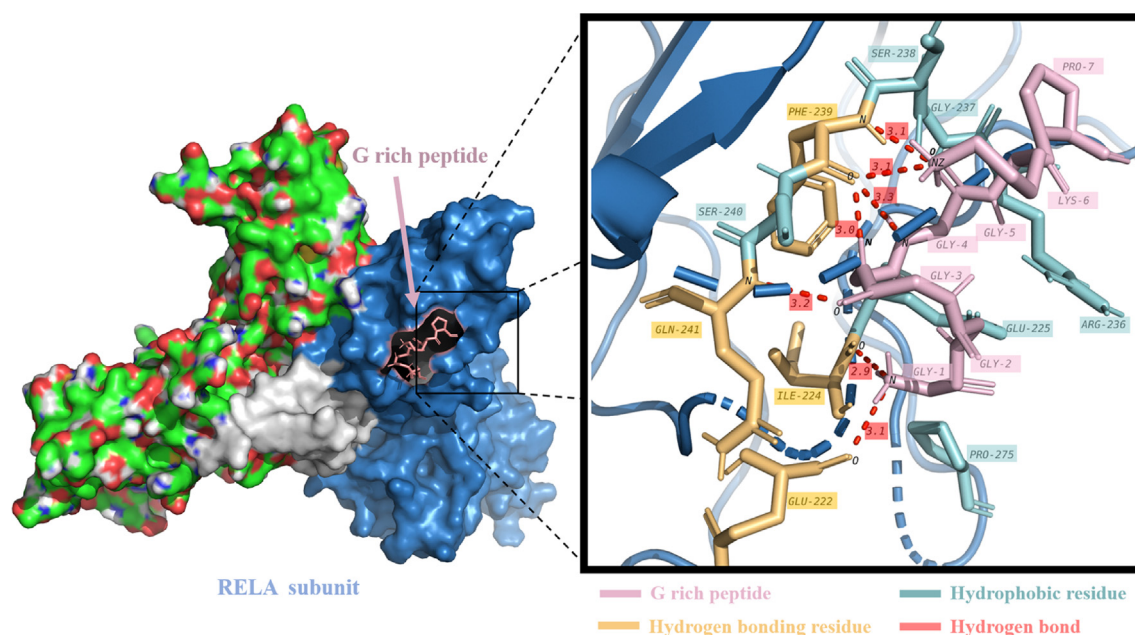

Fig. 4. The molecular docking technique of RELA subunit with G-rich peptide from FCS proteins.

the *IL-1β* gene expression on the PM-MHS model after being treated with G-rich peptide was significantly repressed by 4.17 times compared to that with PM exposure alone. As the expression is associated with NF-κB signaling pathways and inflammatory responses of pathogenic infections [57], the modulation caused by G-rich peptide could be observed in the PM-MHS model. This finding indicates the benefit of G-rich peptide and its potential as anti-inflammatory.
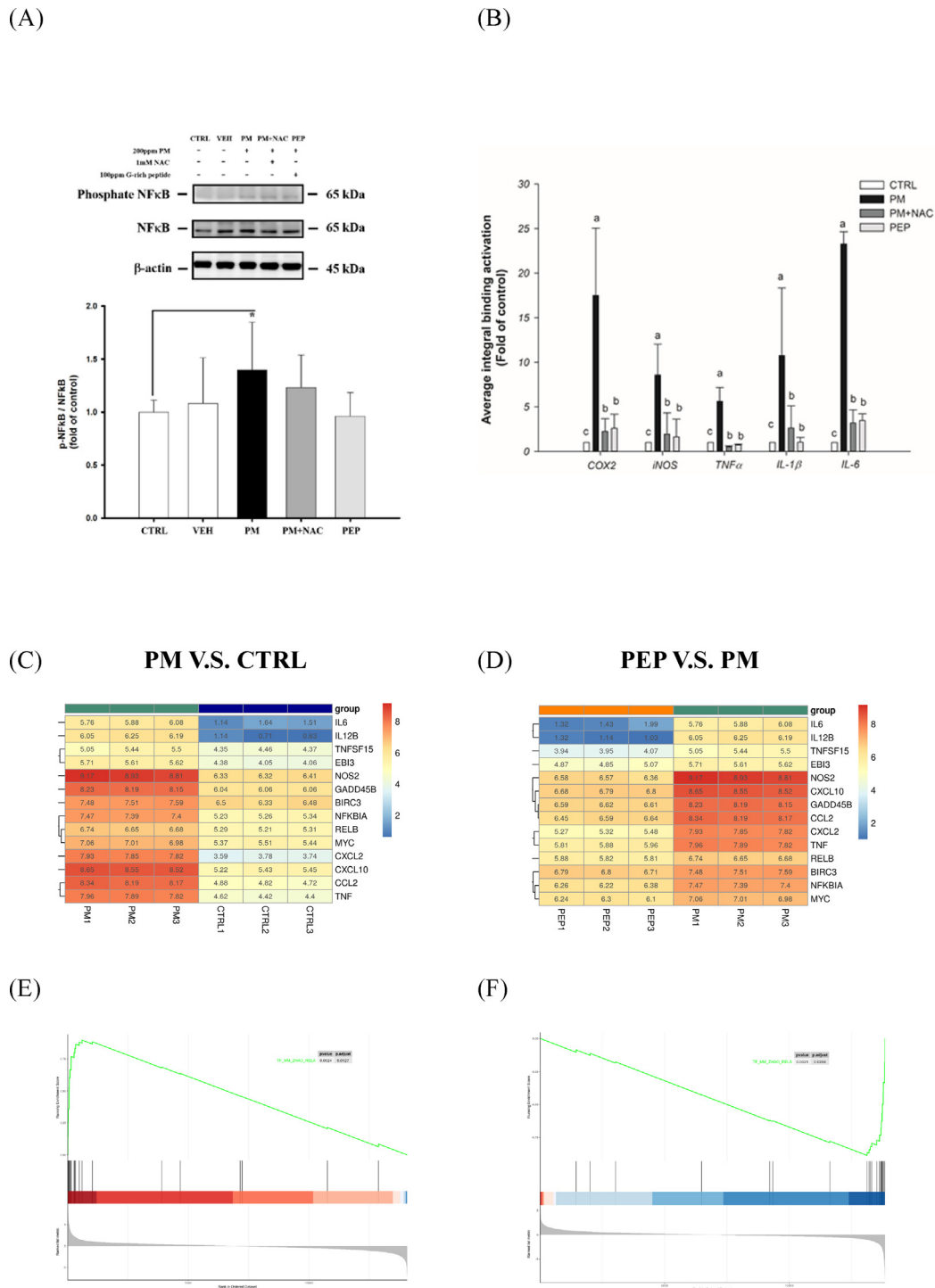

Fig. 5. *The regulatory effect of NF-κB pathway on PM-MHS model. Immunoblot analysis of phosphor−NF−κB/NF-κB ratio (A), Chromatin immunoprecipitation analysis of binding genes of RELA to the promoter regions (B), Heat-map clustering of transcription factor bind profiles in RELA subunit (C, D) and Gene set enrichment analysis (GSEA) (E, F) illustrate PM-induced NF-κB and pro-inflammatory genes. The DEGs with adjusted p-value <0.05 and log2 fold change >1.5 are shown. CTRL: without treatment; PM: treated with only PM (200 ppm) for 24 h; PEP: co-treated with 200 ppm PM and 100 ppm G-rich peptide from FCS proteins for 24 h.*

3.5. Proposed mechanisms of G-rich peptides from MW FCS proteins to modulate PM hazards

Based on the transcriptomic changes observed in PM-MHS model after the treatment of G-rich peptide, the possible mechanisms which regulate NF-κB signaling pathways are proposed. PM could induce an inflammatory response by phosphorylating RELA subunit to activate the NF-κB pathway and its inflammatory factors [58]. Hence, this study investigates the RELA subunit binding ability of the G-rich peptide in NF-κB. Accordingly, the G-rich peptide was found to completely enter the active pockets of the RELA subunit and form 7 hydrogen bonds with a collective affinity value of −5.865 kcal/mol. The hydrogen bonding residues at the active site were Glu-222, Ile-224, Phe-239, Gln-241, and Ser-240, while the hydrophobic binding residues were Glu-224, Arg-236, Gly-237, Ser-238, Ser-240, and Pro-275 (Fig. 4). The binding sites in the RELA subunit are similar to (+)- Betulin as the residues include Glu-222, Ile-224, Phe-239, and Gln-241, and they could also inhibit NF-κB [59]. The result shows that G-rich peptide may have the potential to inhibit RELA phosphorylation.

After treating the PM-MHS cell model with G-rich peptide, the phosphor−NF−κB/NF-κB ratio is significantly decreased by 31.2% compared to the PM-exposed group, as shown in Fig. 5A. Furthermore, ChIP assay analysis revealed that treatment with G-rich peptide leads to a remarkable downregulation in the binding of RELA to the promoter regions of *COX2*, *iNOS*, *TNFα*, *IL-1β*, and *IL-6* genes (Fig. 5B), which are related to the inhibition of ROS production and inflammation. To gain a better understanding of how G-rich peptide represses RELA expression and its effect on RELA-mediated transcription genes, this study investigates the expression of NF-κB transcription factors. Previous studies showed that PM upregulates the expression of chemokine C-X-C-motif ligand 1 (*CXCL1*), *CXCL2*, nitric oxide synthase 2 (*NOS2*), *TNF*, and *IL6*, and in M1-activated macrophage [60]. As shown in Fig. 5C, D, treatment with G-rich peptide significantly represses the expression of these RELA-mediated transcription genes. Furthermore, the transcription gene expression is reversed (Fig. 5E, F), suggesting that it might alleviate PM-induced inflammation through the NF-κB signaling pathway to modulate macrophage polarization.

4. Conclusions

In this study, solid-state fermentation was carried out in a bioreactor in which *R. oligosporus* was utilized to ferment fresh *C. formosanum* sprouts for four days. Afterward, a MWCO protein extraction approach was employed to generate FCS proteins, whereby they were subsequently investigated for their antioxidant capability. The result showed that lower MW FCS proteins (<2 kDa) had stronger antioxidant ability than other higher MW FCS proteins. Specifically, G-rich peptide (GGGGGKP) in the FCS proteins (<2 kDa) revealed the highest ABTS value of 1.01 ± 0.05 mM Trolox. The pharmacokinetic analysis and *in silico* predictions indicated that the G-rich peptide is safe and has negligible effects on inhibiting human xenobiotic metabolism. This study sheds light on the underlying mechanisms of G-rich peptides' effects on NF-κB signaling pathways and immune-related gene ontology by RNA seq. Furthermore, the molecular docking, immunoblots, and ChIP assay analyses confirmed that G-rich peptides from FCS proteins can significantly downregulate the binding of RELA to the promoter regions genes, thereby highlighting its ability as a potential nutraceutical to alleviate oxidative stress and inflammation associated with various diseases.

The present study provides novel insights into the development of food supplements and nutraceuticals from natural proteins as a potential strategy to counteract negative health effects caused by PM. The results of this study may contribute to the development of new functional foods and nutraceuticals with potential health benefits.

Conflicts of interest

The authors declare no conflicts of interest.

Appendix.

Glycine-rich peptides from fermented *C. formosanum* sprout as an antioxidant to modulate the oxidative stress.

Table S1. Specific primers for ChIP analysis.

Cox2_F	5′- CGCAACTCACTGAAGCAGAG - 3′
Cox2_R	5′- CAGTGCTGAGTTCCTTCGTG - 3′
iNOS_F	5′- CAAGCCAGGGTATGTGGTTT - 3′
iNOS_R	5′- CCAGTTGGGTGTGCAAGTTA - 3′
TNFα_F	5′- CACACACACCCTCCTGATTG - 3′
TNFα_R	5′- CTCATTCAACCCTCGGAAAA - 3′
IL1β_F	5′- GGGGGAGCATCCTCATAGA - 3′
IL1β_R	5′- AGGGCACACACAGTATGCAG - 3′
IL6_F	5′- TTCCCATCAAGACATGCTCA - 3′
IL6_R	5′- TCATGGGAAAATCCCACATT - 3′

Table S2. Changes of antioxidant activity of FCS protein.

FCS protein	ABTS (mM Trolox)
Above 10 kDa FCS fraction	0.11 ± 0.03^e
2−10 kDa FCS fraction	0.19 ± 0.03^d
Below 2 kDa FCS fraction	0.23 ± 0.01^c
Below 2 kDa FCS fraction (fraction1)	0.32 ± 0.04^b
G-rich peptide (fraction2)	1.01 ± 0.05^a

Each value represents means $\pm$ SD of 3 replicates.
Data processing was conducted using Microsoft Excel 2016, while SigmaPlot 12.0 (Systat Software, Inc., Chicago, IL, USA) for Windows was employed to carry out Duncan's multiple range and t-tests. Statistical significance was determined at a p-value of less than 0.05. Different letter a-e in the same column means significant difference ($p < 0.05$).
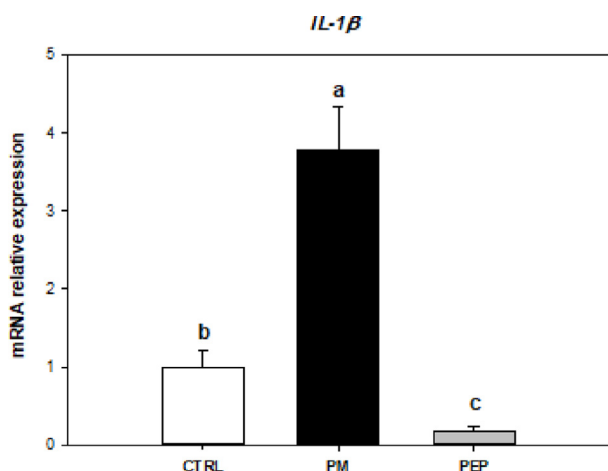

Fig. S1. The mRNA expression of IL1-β on PM-MHS model. Each value represents means $\pm$ SD of 3 replicates. Data processing was conducted using Microsoft Excel 2016, while SigmaPlot 12.0 (Systat Software, Inc., Chicago, IL, USA) for Windows was employed to carry out Duncan's multiple range and t-tests. Statistical significance was determined at a p-value of less than 0.05. Different letter a-c in the same column means significant difference (p < 0.05).

References

[1] Hou CY, Hsieh CC, Huang YC, Kuo CH, Chen MH, Hsieh CW, et al. Development of functional fermented dairy products containing taiwan djulis (Chenopodium formosanum koidz.) in regulating glucose utilization. Fermentation 2022;8:423.

[2] Hsieh CC, Yu SH, Cheng KW, Liou YW, Hsu CC, Hsieh CW, et al. Production and analysis of metabolites from solid-state fermentation of Chenopodium formosanum (djulis) sprouts in a bioreactor. Int Food Res J 2023:112707.

[3] Chen SY, Chu CC, Chyau CC, Yang JW, Duh PD. Djulis (W) and its bioactive compounds affect vasodilation, angiotensin converting enzyme activity, and hypertension. Food Biosci 2019;32:100469.

[4] Li PH, Chan YJ, Hou YW, Lu WC, Chen WH, Tseng JY, et al. Functionality of djulis (Chenopodium formosanum) by-products and in vivo anti-diabetes effect in type 2 diabetes mellitus patients. Biol 2021;10:160.

[5] Guo H, Hao Y, Yang X, Ren G, Richel A. Exploration on bioactive properties of quinoa protein hydrolysate and peptides: a review. Crit Rev Food Sci Nutr 2021;1:14.

[6] Chirinos R, Pedreschi R, Velásquez-Sánchez M, Aguilar-Galvez A, Campos D. In vitro antioxidant and angiotensin I-converting enzyme inhibitory properties of enzymatically hydrolyzed quinoa (Chenopodium quinoa) and kiwicha (Amaranthus caudatus) proteins. Cereal Chem 2020;97:949−57.

[7] Capraro J, De Benedetti S, Di Dio M, Bona E, Abate A, Corsetto PA, et al. Characterization of chenopodin isoforms from quinoa seeds and assessment of their potential anti-inflammatory activity in caco-2 cells. Biomolecules 2020;10:795.

[8] Wu YHS, Chen YC. Trends and applications of food protein-origin hydrolysates and bioactive peptides. J Food Drug Anal 2022;30.

[9] Ye H, Tao X, Zhang W, Chen Y, Yu Q, Xie J. Food-derived bioactive peptides: production, biological activities, opportunities and challenges. J Future Food 2022;2:294−6.

[10] Zhu F. Amaranth proteins and peptides: biological properties and food uses. Food Res Int 2022:112405.

[11] Teixeira CS, Villa C, Sousa SF, Costa J, Ferreira IM, Mafra I. An. In silico approach to unveil peptides from Acheta domesticus with potential bioactivity against hypertension, diabetes, cardiac and pulmonary fibrosis. Food Res Int 2023;169:112847.

[12] Fu H, Liu X, Li W, Zu Y, Zhou F, Shou Q, et al. PM2.5 exposure induces inflammatory response in macrophages via the TLR4/COX-2/NF-κB pathway. Inflammation 2020;43:1948−58.

[13] Kim KE, Cho D, Park HJ. Air pollution and skin diseases: adverse effects of airborne particulate matter on various skin diseases. Life Sci 2016;152:126−34.

[14] Wang J, Huang J, Wang L, Chen C, Yang D, Jin M, et al. Urban particulate matter triggers lung inflammation via the ROS-MAPK-NF-κB signaling pathway. J Thorac Dis 2017;9:4398.

[15] Xin L, Che B, Zhai B, Luo Q, Zhang C, Wang J, et al. 1, 25-dihydroxy vitamin D 3 attenuates the oxidative stress-mediated inflammation induced by PM 2.5 via the p38/NF-κB/NLRP3 pathway. Inflammation 2019;42:702−13.

[16] Sachetto-Martins G, Franco LO, de Oliveira DE. Plant glycine-rich proteins: a family or just proteins with a common motif? Biochim Biophys Acta Gene Regul Mech 2000;1492:1−14.

[17] Mangeon A, Junqueira RM, Sachetto-Martins G. Functional diversity of the plant glycine-rich proteins superfamily. Plant Signal Behav 2010;5:99−104.

[18] Park CJ, Park CB, Hong SS, Lee HS, Lee SY, Kim SC. Characterization and cDNA cloning of two glycine- and histidine-rich antimicrobial peptides from the roots of shepherd's purse, Capsella bursa-pastoris. Plant Mol Biol 2000;44:187−97.

[19] Egorov TA, Odintsova TI, Pukhalsky VA, Grishin EV. Diversity of wheat anti-microbial peptides. Peptides 2005;26:2064−73.

[20] Duong-Ly KC, Gabelli SB. Salting out of proteins using ammonium sulfate precipitation. In: Methods Enzymol, 541. Academic Press; 2014. p. 85−94.

[21] Liu R, Zheng W, Li J, Wang L, Wu H, Wang X, et al. Rapid identification of bioactive peptides with antioxidant activity from the enzymatic hydrolysate of Mactra veneriformis by UHPLC−Q-TOF mass spectrometry. Food Chem 2015;167:484−9.

[22] Ngo DH, Kang KH, Ryu B, Vo TS, Jung WK, Byun HG, et al. Angiotensin-I converting enzyme inhibitory peptides from antihypertensive skate (Okamejei kenojei) skin gelatin hydrolysate in spontaneously hypertensive rats. Food Chem 2015;174:37−43.

[23] Nongonierma AB, Le Maux S, Dubrulle C, Barre C, FitzGerald RJ. Quinoa (*Chenopodium quinoa* Willd.) protein hydrolysates with in vitro dipeptidyl peptidase IV (DPP-IV) inhibitory and antioxidant properties. J Cereal Sci 2015;65: 112−8.

[24] Mudgil P, Kilari BP, Kamal H, Olalere OA, FitzGerald RJ, Gan CY, et al. Multifunctional bioactive peptides derived from quinoa protein hydrolysates: inhibition of α-glucosidase, dipeptidyl peptidase-IV and angiotensin I converting enzymes. J Cereal Sci 2020;96:103130.

[25] Wu CN, Sun LC, Chu YL, Yu RC, Hsieh CW, Hsu HY, et al. Bioactive compounds with anti-oxidative and anti-inflammatory activities of hop extracts. Food Chem 2020;330:127244.

[26] Martinez-Mayorga K, Madariaga-Mazon A, Medina-Franco JL, Maggiora G. The impact of chemoinformatics on drug discovery in the pharmaceutical industry. Expet Opin Drug Discov 2020;15:293−6.

[27] Gupta S, Kapoor P, Chaudhary K, Gautam A, Kumar R. Open Source Drug Discovery Consortium, Raghava, G. P. In silico approach for predicting toxicity of peptides and proteins. PLoS One 2013;8:e73957.

[28] Dimitrov I, Flower DR, Doytchinova I. AllerTOP-a server for in silico prediction of allergens. In: BMC bioinformatics, vol. 14. BioMed Central; 2013. p. 1−9.

[29] Minkiewicz P, Dziuba J, Iwaniak A, Dziuba M, Darewicz M. BIOPEP database and other programs for processing bioactive peptide sequences. J AOAC Int 2008;91:965−80.

[30] Kwon K, Park SH, Han BS, Oh SW, Lee SE, Yoo JA, et al. Negative cellular effects of urban particulate matter on human keratinocytes are mediated by P38 MAPK and NF-κB-dependent expression of TRPV 1. Int J Mol Sci 2018;19:2660.

[31] Lee B, Heo J, Hong S, Kim EY, Sohn YJ, Jung HS. dl-Malic acid as a component of α-hydroxy acids: effect on 2, 4-dinitrochlorobenzene-induced inflammation in atopic dermatitis-like skin lesions in vitro and in vivo. Immunopharmacol Immunotoxicol 2019;41:614−21.

[32] An J, Tang W, Wang L, Xue W, Yao W, Zhong Y, et al. Transcriptomics changes and the candidate pathway in human macrophages induced by different PM2. 5 extracts. Environ Pollut 2021;289:117890.

[33] Tung SY, Lee KC, Lee KF, Yang YL, Huang WS, Lee LY, et al. Apoptotic mechanisms of gastric cancer cells induced by isolated erinacine S through epigenetic histone H3 methylation of FasL and TRAIL. Food Funct 2021;12:3455−68.

[34] Eberhardt J, Santos-Martins D, Tillack AF, Forli S. AutoDock Vina 1.2. 0: new docking methods, expanded force field, and python bindings. J Chem Inf Model 2021;61:3891−8.

[35] Jumper J, Evans R, Pritzel A, Green T, Figurnov M, Ronneberger O, et al. Highly accurate protein structure prediction with AlphaFold. Nature 2021;596:583−9.

[36] Mine Y, Li-Chan E, Jiang B, editors. Bioactive proteins and peptides as functional foods and nutraceuticals, vol. 29. John Wiley & Sons; 2010.

[37] Abbasi S, Moslehishad M, Salami M. Antioxidant and alpha-glucosidase enzyme inhibitory properties of hydrolyzed protein and bioactive peptides of quinoa. Int J Biol Macromol 2022;213:602−9.

[38] Vilcacundo R, Martínez-Villaluenga C, Hernández-Ledesma B. Release of dipeptidyl peptidase IV, α-amylase and α-glucosidase inhibitory peptides from quinoa (*Chenopodium quinoa* Willd.) during in vitro simulated gastrointestinal digestion. J Funct Foods 2017;35:531−9.

[39] Homayouni-Tabrizi M, Asoodeh A, Soltani M. Cytotoxic and antioxidant capacity of camel milk peptides: effects of isolated peptide on superoxide dismutase and catalase gene expression. J Food Drug Anal 2017;25:567−75.

[40] Mirzaei M, Mirdamadi S, Ehsani MR, Aminlari M. Production of antioxidant and ACE-inhibitory peptides from *Kluyveromyces marxianus* protein hydrolysates: purification and molecular docking. J Food Drug Anal 2018;26:696−705.

[41] Wu HC, Pan BS, Chang CL, Shiau CY. Low-molecular-weight peptides as related to antioxidant properties of chicken essence. J Food Drug Anal 2005;13:11.

[42] Farvin KS, Andersen LL, Otte J, Nielsen HH, Jessen F, Jacobsen C. Antioxidant activity of cod (*Gadus morhua*) protein hydrolysates: fractionation and characterization of peptide fractions. Food Chem 2016;204:409−19.

[43] Nwachukwu, Aluko D, Rotimi E. Structural and functional properties of food protein-derived antioxidant peptides. J Food Biochem 2019;43:e12761.

[44] Gangopadhyay N, Hossain MB, Rai DK, Brunton NP. A review of extraction and analysis of bioactives in oat and barley and scope for use of novel food processing technologies. Mol 2015;20:10884−909.

[45] Majumder K, Mine Y, Wu J. The potential of food protein-derived anti-inflammatory peptides against various chronic inflammatory diseases. J Sci Food Agric 2016;96:2303−11.

[46] Ren LK, Yang Y, Ma CM, Fan J, Bian X, Liu BX, et al. Identification and in silico analysis of novel antioxidant peptides in broken rice protein hydrolysate and its cytoprotective effect against H2O2-induced 2BS cell model. Food Res Int 2022; 162:112108.

[47] Chen Y, Kwon SW, Kim SC, Zhao Y. Integrated approach for manual evaluation of peptides identified by searching protein sequence databases with tandem mass spectra. J Proteome Res 2005;4:998−1005.

[48] Guru A, Lite C, Freddy AJ, Issac PK, Pasupuleti M, Saraswathi NT, et al. Intracellular ROS scavenging and antioxidant regulation of WL15 from cysteine and glycine-rich protein 2 demonstrated in zebrafish in vivo model. Dev Comp Immunol 2021;114:103863.

[49] Wong FC, Ong JH, Kumar DT, Chai TT. In silico identification of multi-target anti-SARS-CoV-2 peptides from quinoa seed proteins. Int J Pept Res Ther 2021;27:1837−47.

[50] Santos GB, Ganesan A, Emery FS. Oral administration of peptide-based drugs: beyond Lipinski's Rule. ChemMedChem 2016;11:2245−51.

[51] Raghav PK, Verma YK, Gangenahalli GU. Peptide screening to knockdown Bcl-2's anti-apoptotic activity: implications in cancer treatment. Int J Biol Macromol 2012;50:796−814.

[52] ISO 10993-5:2009 biological evaluation of medical devices. Part 5: tests for in vitro cytotoxicity; international organization for standardization. 2009. Geneva, Switzerland.

[53] Phongthai S, Rawdkuen S. Fractionation and characterization of antioxidant peptides from rice bran protein hydrolysates stimulated by in vitro gastrointestinal digestion. Cereal Chem 2020;97:316−25.

[54] Cao Z, Liao Q, Su M, Huang K, Jin J, Cao D. AKT and ERK dual inhibitors: the way forward? Cancer Lett 2019;459: 30−40.

[55] Wang J, Huang J, Wang L, Chen C, Yang D, Jin M, et al. Urban particulate matter triggers lung inflammation via the ROS-MAPK-NF-κB signaling pathway. J Thorac Dis 2017;9: 4398.

[56] Lee CW, Vo TTT, Wu CZ, Chi MC, Lin CM, Fang ML, et al. The inducible role of ambient particulate matter in cancer progression via oxidative stress-mediated reactive oxygen species pathways: a recent perception. Cancers 2020;12:2505.

[57] Fernando I, Kim HS, Sanjeewa K, Oh JY, Jeon YJ, Lee WW. Inhibition of inflammatory responses elicited by urban fine dust particles in keratinocytes and macrophages by diphlorethohydroxycarmalol isolated from a brown alga *Ishige okamurae*. ALGAE 2017;32:261−73.

[58] Zhang ZB, Luo DD, Xie JH, Xian YF, Lai ZQ, Liu YH, et al. Curcumin's metabolites, tetrahydrocurcumin and octahydrocurcumin, possess superior anti-inflammatory effects in vivo through suppression of TAK1-NF-κB pathway. Front Pharmacol 2018;9:1181.

[59] Anaya-Eugenio GD, Eggers NA, Ren Y, Rivera-Chávez J, Kinghorn AD, de Blanco EJC. Apoptosis induced by (+)-Betulin through NF-κB inhibition in MDA-MB-231 breast cancer cells. Anticancer Res 2020;40:6637−47.

[60] Shi Q, Zhao L, Xu C, Zhang L, Zhao H. High molecular weight hyaluronan suppresses macrophage M1 polarization and enhances *IL-10* production in PM2.5-induced lung inflammation. Molecules 2019;24:1766.